Journal of Experimental Nanoscience

ISSN: 1745-8080 (Print) 1745-8099 (Online) Journal homepage: informahealthcare.com/journals/tjen20

Ultrafine titanium dioxide nanoparticles induce cell death in human bronchial epithelial cells

Eric Chen, Miguel Ruvalcaba, Lindsey Araujo, Ryan Chapman & Wei-Chun Chin

To cite this article: Eric Chen, Miguel Ruvalcaba, Lindsey Araujo, Ryan Chapman & Wei-Chun Chin (2008) Ultrafine titanium dioxide nanoparticles induce cell death in human bronchial epithelial cells, Journal of Experimental Nanoscience, 3:3, 171-183, DOI: 10.1080/17458080802412430

To link to this article: https://doi.org/10.1080/17458080802412430

Published online: 27 Sep 2008.

Submit your article to this journal

Article views: 891

View related articles

Citing articles: 1 View citing articles

Full Terms & Conditions of access and use can be found at
https://informahealthcare.com/action/journalInformation?journalCode=tjen20

Journal of Experimental Nanoscience
Vol. 3, No. 3, September 2008, 171–183

Taylor & Francis
Taylor & Francis Group

Ultrafine titanium dioxide nanoparticles induce cell death in human bronchial epithelial cells

Eric Chen, Miguel Ruvalcaba, Lindsey Araujo, Ryan Chapman and Wei-Chun Chin*

School of Engineering, University of California, Merced, CA, USA

(*Received 31 March 2008; final version received 15 August 2008*)

Titanium dioxide (TiO_2) nanoparticles (TNPs), once perceived as harmless, have been shown to induce cytotoxicity on various cell types under UV radiation. However, whether TNPs elicit cell death in the absence of UV has not been thoroughly studied. This study aims to investigate the TNPs-induced cell death mechanism in UV-absent condition by examining the reduction of cell viability and apoptotic cell death characteristics in the human bronchial epithelial cell line, Chago-K1. The Chago-K1 cells were exposed to TNPs for 24 h at concentrations ranging from 0.1 to 2 mg mL^{-1}. CCK-8 and Live/Dead assays demonstrating diminishing cell viability indicate that peak cell death occurred around 2 mg mL^{-1} TNPs after 24 h treatment in darkness. Apoptotic related cell death mechanisms were demonstrated by chromatin condensation and translocation of phosphatidylserine with Annexin V staining. Here we demonstrate that ultrafine TNPs (75 nm) in darkness can induce significant cytotoxicity on the Chago-K1 cells possibly through apoptotic pathways.

Keywords: titanium dioxide; nanoparticle; UV-absent nanotoxicity; airway cells

1. Introduction

Titanium dioxide (TiO_2) exists naturally in the form of minerals such as rutile and anatase [1,2]. Traditionally, TiO_2 has been commonly accepted as a biologically inert substance to both animals and humans [3–7]. As a consequence, it is utilised widely in commercial products such as paints, cosmetics, textiles, papers, plastics, sunscreens and food [8–10].

Titanium dioxide nanoparticles (TNPs) are added to many commercial products; however, little is known about the environmental and health implications of their use. Due to their photocatalytic activity, one of the environmental applications of TNPs involves effective catalysis of decomposing organic contaminants found in water and aqueous wastes [11,12]. The mechanism of this reaction involves the absorption of UVA by TNPs to catalyse the production of reactive oxygen species (ROS), mainly hydroxyl radicals, superoxide ions, and hydrogen peroxide in aqueous phase [13–16]. Recent advances in the photocatalytic capability of TNPs have also shed light on novel applications for photodynamic therapy for endobronchial cancers [17].

*Corresponding author. Email: wchin2@ucmerced.edu

ISSN 1745–8080 print/ISSN 1745–8099 online
© 2008 Taylor & Francis
DOI: 10.1080/17458080802412430
http://www.informaworld.com

Evidence has shown that exposure to TNPs and UV radiation destroys cells by generating oxidative stress and catalysing the production of ROS [13,18], but little is known of the cytotoxicity of TNPs in the absence of UV light. Despite conflicting data suggesting the harmlessness of TNPs on animal and human cells in the absence of photoactivation from UV radiation [19–23], a steady increase in studies substantiating chronic pulmonary inflammation in the rat [24] and proinflammatory effects in human endothelial cells without UV activation is emerging [25]. Studies have subsequently observed that TNP exposure can destroy airway epithelium, impair macrophage phagocytotic function, induce recruitment of neutrophils [26] and cause airway inflammation and allergic airway sensitisation [27]. For both human and rat alveolar macrophage, exposure to TNPs leads to the augmented production of ROS [1]. TNP cytotoxicity is further exhibited by apoptotic cell death as indicated by the formation of apoptotic bodies and DNA fragmentation in Syrian hamster embryo fibroblasts [1].

Since TNPs have become a common component in the manufacturing of various products, the possibility of human exposure is realistic. Therefore, it is important to investigate the potential health threats that these particles may pose. In this study we report that TNPs (75 nm) can induce cytotoxicity in airway bronchial epithelial cells in the absence of UV photoactivation. Our data suggest that the observed TNP-induced cell death takes place through an apoptotic mechanism.

2. Materials and methods

2.1. *Culture of epithelial cells*

The human airway bronchial epithelial cell line Chago-K1 was obtained from American Type Culture Collection (ATCC, Manassas, VA, USA). Cells were cultured in 15 cm cell culture plates (Falcon, VWR, CA, USA) in RPMI 1640 medium (RPMI 1640, Invitrogen, CA, USA) supplemented with L-glutamine, 1% penicillin/streptomycin and 10% heat inactivated fetal bovine serum (FBS). Cultures were incubated in a humidified incubator at 37°C/5% CO_2. Cell counts were performed using trypan blue (Sigma-Aldrich, St. Louis, MO, USA) exclusion and a Bright-Line haemocytometer.

2.2. *Particles*

The nanoparticles used in this study were ultrafine nanoparticle titanium (IV) dioxide (<75 nm, mixture of rutile and anatase) (Sigma-Aldrich, St. Louis, MO, USA). The 5 wt% dispersion in water stock solution was reconstituted into a 10 mg mL^{-1} concentration using RPMI 1640 medium containing no FBS.

2.3. *Cell treatments*

Cells were seeded at 1.5×10^5 cells per well in a 24-well plate and incubated for 24 h in RPMI 1640 supplemented with 10% FBS. After 24 h growth, the cells reached $\approx$70% confluence and were rinsed with phosphate buffered saline (PBS) and then replaced with the appropriate concentrations of TNPs before incubation for a further 24 h.

The concentrations of 0.1, 0.3, 0.5, 0.7, 1 and 2 mg mL^{-1} TNPs in serum-free RPMI were prepared and thoroughly mixed before being added to each well. The concentration range used here is consistent with many published reports [18,28–30]. Following 24 h particle treatments, the FBS-free medium was removed from the cells and the culture was rinsed with Hank's Buffer Salt Solution (HBSS, Invitrogen, CA, USA). Each experiment was repeated independently for three times in 24-well plates.

2.4. *CCK-8 assay*

Photocolourimetric determination of cytotoxicity was assessed using CCK-8 dye (Dojindo Laboratories, Tokyo, Japan). CCK-8, being non-radioactive, offers a colourimetrical determination of the percentage of viable cells subjected to varying TNP concentrations. This assay kit measures the metabolic activity of dehydrogenases within the viable cells to convert WST-8 Tetrazolium salt into water-soluble formazan. It was prepared by adding CCK-8 in HBSS, enough for 24-well plates in a 1 : 10 dilution. Cells were rinsed with HBSS and 200 μL of the dye was loaded into each well and incubated in a 37°C, 5% CO_2 incubator for 1 h. The absorbance was measured by using Thermo Multiscan EX plate reader (Thermo Multiskan EX plate reader, VWR, CA, USA) at the optical density of 450 nm (650 nm reference). An average was calculated from three separate data sets for each concentration, including the untreated control, from three independent experiments and was tabulated as a percentage of the untreated control. The cell viability was calculated by $\{(OD_{450\text{treatment}} - OD_{650\text{treatment}})/(OD_{450\text{control}} - OD_{650\ \text{control}}) \times 100\%\}$.

2.5. *Live/Dead assay*

Live/Dead Viability/Cytotoxicity assay dye (Live/Dead Viability/Cytotoxicity Assay Kit, Invitrogen, CA, USA) was prepared by adding 10 μL of 2 mM EthD-1 stock solution and 2.5 μL of 4 mM calcein AM stock solution to 10 mL of HBSS in a 15 mL tube. The staining solution (200 μL) was added to each well and the plate was incubated at room temperature for 45 min prior to image acquisition. Upon image analysis using Simple PCI (Compix Inc., Imaging Systems, Sewickle, PA, USA), three independent images were taken in each well for each concentration at 200× magnification. In each image, the total visible stained cells were counted. The number of dead and viable cells visible through the Live/Dead Assay was compared to the total number of visible cells in the control.

2.6. *Hoechst/Cell tracker staining*

Hoechst/Cell tracker assay dye (Molecular Probes, Invitrogen, CA, USA) was prepared by making a final concentration of 5 μg mL^{-1} Hoechst stock solution and 10 μM of Cell tracker dye in HBSS. Aliquots of this solution (200 μL) were added to wells on the plate. The plate was placed in a 37°C/5% CO_2 incubator for 20 min. Upon image analysis using SimplePCI (Compix Inc., Imaging Systems, Sewickle, PA, USA), three independent images were taken in each well for each concentration at 200 × magnification. For each image, the number of cells containing chromatin condensation made visible through

Hoechst staining was compared to the total number of cells stained with Cell tracker dye. Only brightly fluorescent blue dots were counted as condensed chromatin. Ratios were tabulated for each concentration and were subsequently compared to the untreated control. Final results were calculated and presented as chromatin condensation percentages for each TiO_2 concentration of the control.

2.7. *Hoechst/Annexin V staining*

Hoechst/Annexin V assay (Molecular Probes, Invitrogen, CA, USA) dye was prepared by adding 2.5 μL of Annexin V Alexa Fluor® 488 conjugate stock solution in 100 μL of Annexin binding buffer. The solution was then supplemented with 2.5 μL of Hoechst stock solution for every 1000 μL of the Annexin binding buffer, making a final concentration of 5 μg mL^{-1} Hoechst dye. Annexin binding buffer was composed of 10 mM HEPES, 140 mM NaCl, and 2.5 mM $CaCl_2$ at pH 7.4. Prior to staining, cells were rinsed with HBSS. Annexin binding buffer (200 μL) with Hoechst and Annexin V dyes were placed in each well and incubated at room temperature for 15 min.

2.8. *Image analysis*

After staining the treated cells, image analysis was performed with an inverted Nikon Eclipse TE2000-U fluorescent microscope (Nikon Eclipse TE2000-U, Tokyo, Japan). Each photo was taken at a magnification of 200× and analysed using the imaging analysis system, SimplePCI (Compix Inc., Imaging Systems, Sewickle, PA, USA). The data were based on multiple photos; each contained roughly 100–200 cells, which were counted individually resulting in an overall percentage.

2.9. *Statistical analysis*

Data were presented as means ± SD. Each experiment was performed independently at least three times. Statistical significance was determined using a Student's *t*-test analysis with p values of <0.005 (GraphPad Prism 4.0, GraphPad Software, Inc., San Diego, CA, USA).

3. Results

3.1. *TNP-induced decrease in cell viability*

In order to assess TNP toxicity on airway bronchial epithelial cells, cell culture experiments using Chago-K1 bronchus carcinoma were performed. The cytotoxic effect was first evaluated by the Cell Counting Kit-8 (CCK-8) assay. A dose-dependent decline in cell viability was observed with each increment in TNP concentration (Figure 1). The highest 2 mg mL^{-1} TNP concentration showed significant cytotoxicity by reducing the cell survival to 65% while the control group did not experience any significant decrease in viable cell numbers. Low dosages of TNP concentration (0.1–0.3 mg mL^{-1}) also appear to show significant cytotoxicity compared with the control. The data indicate that TNPs can induce a significant reduction of cell viability.

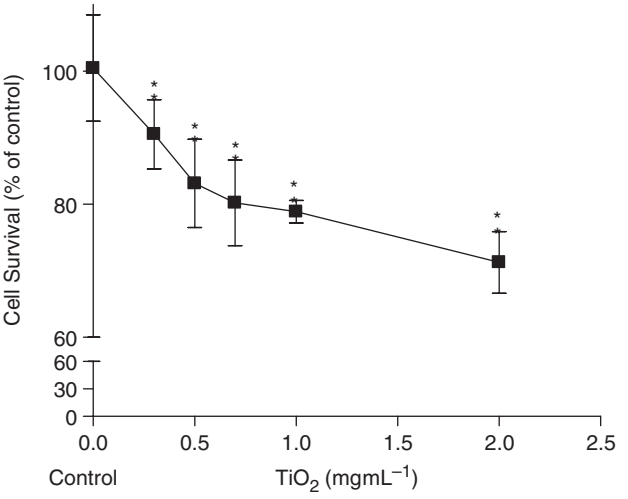

Figure 1. Relative cell viability of Chago-K1 cells monitored by CCK-8 assay following 24 h exposure to various TiO_2 concentrations. Data are shown as percentages of viability in comparison with untreated control and presented as mean ± SD of three separate experiments. Treated groups are significantly different from the untreated control at $p < 0.005$ as indicated by '**'.

3.2. *TiO_2-induced increase in cell death*

The Live/Dead Viability/Cytotoxicity Assay Kit was used to confirm cytotoxic effects of TNPs on Chago-K1 cells (Figure 2) that were observed using the CCK-8 assay. Dead cells were stained with red ethidium homodimer dye and the live cells were stained with green calcein AM (revealing red and green stains, respectively). Both live and dead cells followed a dose-dependent trend upon treatment with nanoparticles, demonstrating the greatest cell death (34%) at $2\,mg\,mL^{-1}$. Dead cells were found at a significantly higher density in greater TNP concentrations ($1–2\,mg\,mL^{-1}$) while live cells were found at higher density (83% and 95%) in lower concentrations of TNPs (0.3 and $0.1\,mg\,mL^{-1}$). Cells loaded with red and green dyes were viewed under an inverted microscope at 488 and 630 nm wavelengths. The results showed that TNPs can induce cytotoxic effects on bronchus carcinoma, Chago-K1 cells.

3.3. *TiO_2-induced nuclear and membrane changes associated with apoptosis*

Hoechst staining was used to measure the potential of TNPs to induce nuclear changes involving chromatin condensation that are characteristic of apoptosis [1]. Hoechst is a cell permeant dye that binds to DNA and fluoresces brightly blue [1]. The untreated control did not show the characteristic apoptotic nuclear changes (Figure 4(h)). Characteristic apoptotic structures (apoptotic bodies) within nuclei were clearly revealed and quantified after 24 h of TNP treatment (Figures 3 and 4(b) and 4(e)). Cytotoxicity was indicated by a positive correlation between TNP concentrations and apoptotic bodies (Figure 3). The steep rise in chromatin compaction occurred between the concentrations of 0.3 and $1\,mg\,mL^{-1}$ and began to plateau as the concentrations exceeded $1–2\,mg\,mL^{-1}$.

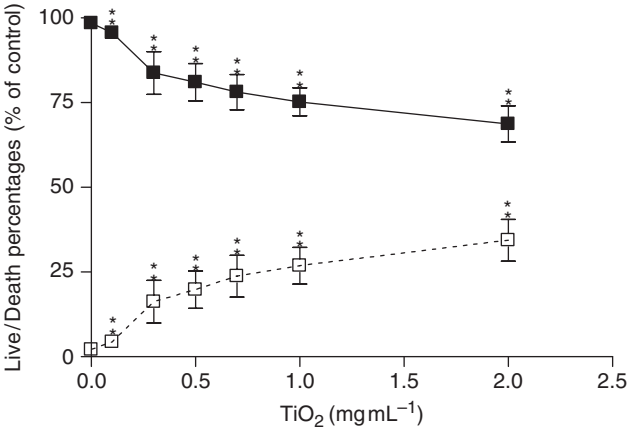

Figure 2. Percentages of cell alive/dead (Chago-K1 cells) detected using Live/Dead assay kit following exposure to various concentrations of TiO_2 for 24 h. Solid squares symbolise the percentages of live cells while the open squares correspond to the percentages of dead cells. Data are presented as Live/Dead percentages of the untreated control and displayed as mean±SD of three separate experiments. Treated groups are significantly different from the untreated control at $p < 0.005$ as indicated by '**'.

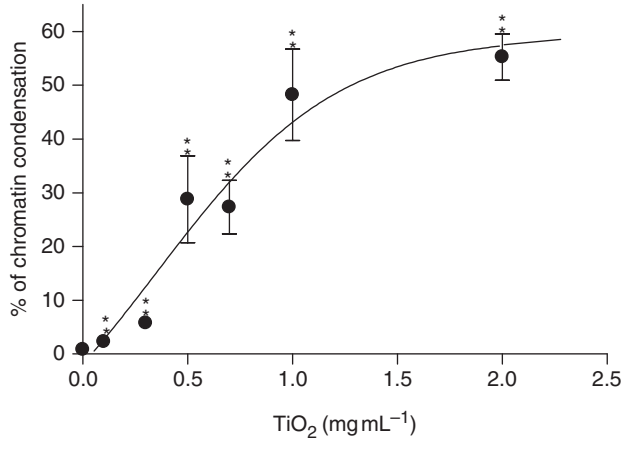

Figure 3. Percentages of chromatin condensation detected by Hoechst dye staining following exposure to different TiO_2 concentrations for 24 h. Data are presented as percentages of chromatin condensation in comparison with the untreated control and displayed as mean±SD of three separate experiments. Treated groups are significantly different from untreated control at $p < 0.005$ as indicated by '**'.

TNP-induced cytotoxicity was further corroborated by phosphatidylserine translocation from the inner to outer leaflet of cell membrane, another apoptosis characteristic [31]. In this study, externalisation of phosphatidylserine was identified by green Annexin V staining. Concurrently, Annexin V positive cells were stained with Hoechst dye which revealed co-localised fluorescence of chromatin condensation in the nucleus and Annexin V

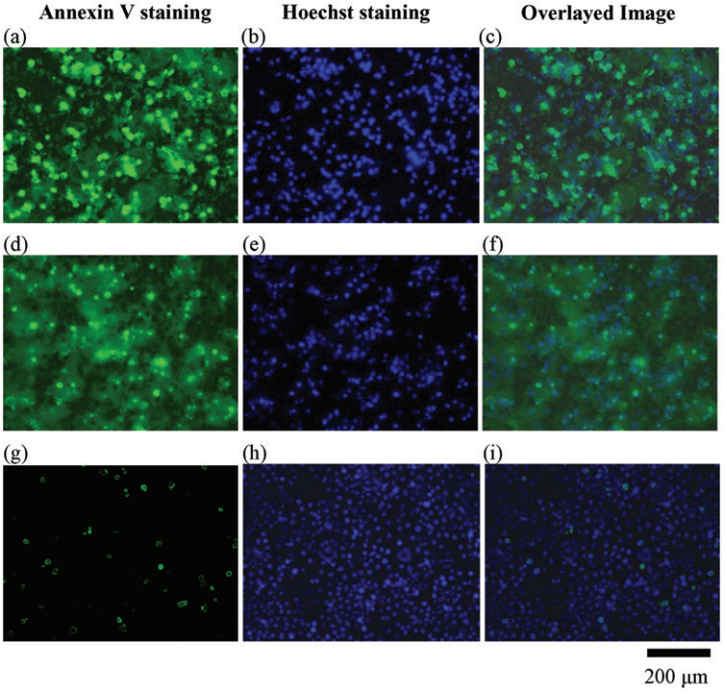

Figure 4. Images of fluorescent staining of Annexin V, Hoechst and overlay in Chago-K1 cells following 24 h treatment of different TiO_2 concentrations. Cell nuclei were stained light blue by Hoechst dye in the untreated control group but appeared rounded and brightly fluorescent in the treated groups. The green Annexin V staining clearly labelled cell membrane confirming translocation of phosphatidylserine from the inner to outer leaflet of cell membrane. (a)–(c) Treatment of $1\,mg\,mL^{-1}$ TiO_2 in Chago-K1 cells. (d)–(e) Treatment of $0.3\,mg\,mL^{-1}$ TiO_2 also revealed significant increase in Annexin V and Hoechst staining compared to the control (no nanoparticles) (g)–(i).

around membrane within a single cell. The co-localised signals also increased in relation to the elevated TNP dosages providing further evidence for possible apoptotic mechanism as exhibited by Figure 4(a)–(i). Consistent with Hoechst staining, such co-localisation signals increased at 24 h with higher concentrations of TNPs (Figures 3 and 4(a)–(i)).

4. Discussion

Understanding the toxicological effects that TNPs induce on human airway epithelial cells is essential to the understanding of TNPs-caused airway-related diseases, abnormal development of airway epithelium, and the establishment of a safety standard for TNP waste disposal [32–38]. It has already been suggested that nanoparticles have a high propensity to be inhaled and deposited in the pulmonary system [39,40]. Chago-K1, a human bronchial epithelial cell line, appears to be a good model that mimics the possible targeted nanotoxicological TNP-induced injury [7]. Therefore, this study aims to

investigate the role of TNPs on activating apoptotic pathways in human bronchial epithelial cell line Chago-K1.

Many published reports have validated the exposure of TNP-induced cytotoxicity, apoptosis and inflammation responses in various cell types including the mesenchymal stem cell [41], lymphoblastoid cells [42], alveolar epithelial cell of the lung [43,44], alveolar macrophages [45], phagocytes [46], colon cells [18] and osteoblast [47]. Additionally, previous studies have shown that titanium dioxide, a highly potent photocatalytic substance when exposed to UV radiation, exhibits disinfection ability [13,48], which contributes to a better understanding of the cytotoxicity of TNPs. Previous reports have found that TNP cytotoxicity cannot be generated in the absence of UV irradiation or with UV irradiation alone [19–21]. On the contrary, Gurr et al. [7] demonstrated that treatments with 10 and 20 nm anatase TNPs ($10\,\mu g\,mL^{-1}$) for 1 h induced significant oxidative stress-related cellular damage in the absence of photocatalysis such as lipid peroxidation, oxidative DNA damage and elevated levels of nitric oxide and hydrogen peroxide [7]. According to the report, however, larger TiO_2 particles ($\geq$200 nm) failed to induce oxidative stress-related cytotoxicity. Anatase and rutile mixed TNPs were able to induce higher oxidative DNA damage than either pure anatase or rutile form [7]. Even though the entry, uptake, accumulation and distribution of TNPs in tissue such as rat tracheal explants have been demonstrated, [49] the mechanism of TNP-induced airway epithelial cell death has not been thoroughly investigated.

In our current study, 75 nm TNPs were used with a mixture of anatase and rutile form. The selected size range represents a particle size that is midway between 10–20 nm and 100–200 nm and is usually neglected in most studies. Since a mixture of rutile and anatase has been suggested to produce more profound cellular damage [7], this mixture was chosen to study TiO_2 cytotoxic mechanisms. The treatment of TNPs for 24 h yielded a significant decrease in the viability of Chago-K1 cells that was indicated by the CCK-8 and Live/Dead assays (Figures 1 and 2). A similar reduction in viable cell number was observed by Gurr et al. [7]. In that study, bronchial epithelial cells cultured with 10 nm TNPs at $1\,\mu g\,mL^{-1}$ for 3 days retarded cell growth by $\approx$30%. Our results showed a maximum amount of dead cells at roughly 34%; however, that was only attained at the highest 75 nm TNP concentration used ($2\,mg\,mL^{-1}$). The difference in cytotoxicity could possibly be explained by the differential nanotoxicity effects based on different size range. The smaller TNPs have been suggested to cause more oxidative stress and cytotoxicity as a result of having large surface area-to-volume ratio [7,29]. Similar dose-dependent cytotoxicity and cell death induced by TNPs in the absence of UV photoactivation have also been found with comparable range of TNP concentrations ($0.03–2\,mg\,mL^{-1}$) [29]. Higher percentages of cell death were found by Barlow et al. [29]; however, the 29 nm TNPs used in that study were smaller than the 75 nm TNPs used in this study which might have accounted for the increased cell death observed in their results. Other investigations on nanotoxicity reported that the treatment of 40 nm TNPs for 48 h (without UV) on the neuroblatoma-2A (N2A) cell line were also similar to our results [50]. Jeng and Swanson [50] found an $\approx$10% reduction in N2A viability at $0.1\,mg\,mL^{-1}$ while $0.2\,mg\,mL^{-1}$ yielded roughly 25% drop in cell viability. We found roughly 5% ($0.1\,mg\,mL^{-1}$) and 16% ($0.3\,mg\,mL^{-1}$) death rates that are consistent with the report from Jeng and Swanson [50]. When considering TNP nanotoxicity under UV photoactivation, Zhang and Sun [18] described that a rapid decline in viable cells was observed when colon cancer cell line (Ls-174-t) was incubated with

21.1 nm TNPs with UV photoactivation. In their study, 0.2 mg mL^{-1} TNPs reduced percentages of cell survival from 100 to 80% within 30 min while 1 mg mL^{-1} resulted in a drop from 100 to ≈20% in the same length of time. The difference in toxicity between the presence and the absence of UV exposure implies a possible cytotoxicity mechanism that is independent of ROS production from UV.

The high dosages of TNPs (1–2 mg mL^{-1}) used in our experiment might not be experienced in the airway under normal exposure conditions but were included for a complete evaluation of TNP toxicity. Although our results may exhibit an accurate representation of TNP-induced cell death and cytotoxicity by measuring the concentration of formazan dye (as an indication of viable cells), possible interference from TNPs could affect the colourimetric absorbance reading as TNPs are known to scatter light. To minimise the effects of interference, additional measurements were made in a reference wavelength at 650 nm which represents the light scattered by TNPs. Subtracting the readings taken at 650 nm from the readings at 450 nm provides the actual concentration of formazan dye.

Identification of apoptotic markers is necessary to determine whether apoptosis is the mechanism for TNP-induced cell death. The characteristic morphology of apoptosis-induced cell death include cell shrinkage, compaction and condensation of chromatin toward the nuclear periphery, DNA fragmentation, and translocation of phospholipids from inner to outer leaflet of the cell membrane [1,51–53]. Demonstration of more than one of these parameters is needed to verify that the apoptosis-induced cell death mechanism is generated by TNPs. In our experiment, utilisation of Annexin V stain confirmed the translocation of phosphatidylserine from the inner to the outer leaflet of the cell membrane at higher TNP concentrations. This result was subsequently superimposed with Hoechst signal which represents the cardinal features of apoptotic nuclear damage such as chromatin condensation and marginalisation when exposed to TNPs (Figure 4). It was clearly shown that higher concentration of TNPs at 1 mg mL^{-1} yielded more Annexin V and Hoechst co-localised staining than with the 0.3 mg mL^{-1} treatment. Hence, we suggest that TNPs are capable of inducing cell death in human bronchial epithelial cell via a possible apoptotic pathway in the absence of UV.

In further confirmation of a UV-independent apoptotic pathway in human bronchial epithelial cells, the Hoechst data revealed a significant increase in chromatin condensation proportional to the rise in TNP concentrations (Figure 3). At the same time, the percentages of chromatin condensation are reflected by the increase of apoptosis-instigated cells. Our results were also comparable to similar research investigating TNP-dependent chromatin condensation in Syrian hamster embryo fibroblasts [1]. Despite the usage of <20 nm TNPs at lower dosages (from 0.5 μg cm^{-2} to 5 μg cm^{-2}), that study found a general trend displaying elevated numbers of apoptotic bodies with increasing TNP concentration after 24 h treatment [1]. A slight plateau began at 1–2 mg mL^{-1} in our results. This phenomenon may be explained by an unequal distribution of TNPs at high concentrations as particle aggregations tend to form larger particles generating a range of TNP sizes that complicate the degree of cytotoxicity [7,49]. A possible solution is the sonication of TNPs before treatment to avoid aggregation [30]. However, because chromatin compaction may occur prior to cell death, as mitochondrial dehydrogenase activity is still functional, measurements of chromatin compaction at 24 h may not precisely reflect CCK-8 and Live/Dead Assay data. Should the treatment time be extended

to 36 h or 48 h, the number of apoptotic bodies can be expected to coincide better with cell death and viability. Given the two independent proofs of chromatin condensation and translocation of phosphatidylserine, apoptosis is a likely cell death mechanism induced by TNPs.

To our knowledge this is the first study suggesting the apoptotic pathway in TNP-induced cytotoxicity on airway bronchial epithelial cells. Our results also provide evidence that inhalation of TNPs cause direct intratracheal cell death via possible apoptotic mechanisms. Further investigation into the apoptotic signalling pathway induced by TNPs is essential for a more in-depth understanding of other possible toxic effects of TNPs.

Acknowledgements

EC, WCC, MR and LA were supported by CITRIS and NSF CINS programme while working on this project.

References

[1] Q. Rahman, M. Lohani, E. Dopp, H. Pemsel, D.G. Weiss, and D. Schiffmann, *Evidence that ultrafine titanium dioxide induces micronuclei and apoptosis in Syrian hamster embryo fibroblasts*, Environ. Health Perspect. 110(8) (2002), pp. 797–800.

[2] M. Hedenborg, *Titanium dioxide induced chemiluminescence of human polymorphonuclear leukocytes*, Int. Arch. Occup. Environ. Health 61(1–2) (1988), pp. 1–6.

[3] B.K. Bernard, M.R. Osheroff, A. Hofmann, and J.H. Mennear, *Toxicology and carcinogenesis studies of dietary titanium dioxide-coated mica in male and female Fischer 344 rats*, J. Toxicol. Environ. Health 29(4) (1990), pp. 417–429.

[4] J.L. Chen and W.E. Fayerweather, *Epidemiologic study of workers exposed to titanium dioxide*, J. Occup. Med. 30(12) (1988), pp. 937–942.

[5] G.A. Hart and T.W. Hesterberg, *In vitro toxicity of respirable-size particles of diatomaceous earth and crystalline silica compared with asbestos and titanium dioxide*, J. Occup. Environ. Med. 40(1) (1998), pp. 29–42.

[6] R.C. Lindenschmidt, K.E. Driscoll, M.A. Perkins, J.M. Higgins, J.K. Maurer, and K.A. Belfiore, *The comparison of a fibrogenic and two nonfibrogenic dusts by bronchoalveolar lavage*, Toxicol. Appl. Pharmacol. 102(2) (1990), pp. 268–281.

[7] J.R. Gurr, A.S. Wang, C.H. Chen, and K.Y. Jan, *Ultrafine titanium dioxide particles in the absence of photoactivation can induce oxidative damage to human bronchial epithelial cells*, Toxicology 213(1–2) (2005), pp. 66–73.

[8] K.E. Levine, R.A. Fernando, M. Lang, A. Essader, and B.A. Wong, *Development, and validation of a high-throughput method for the determination of titanium dioxide in rodent lung and lung-associated lymph node tissues*, Anal. Lett. 36(3) (2003), pp. 563–576.

[9] C. Gelis, S. Girard, A. Mavon, M. Delverdier, N. Paillous, and P. Vicendo, *Assessment of the skin photoprotective capacities of an organo-mineral broad-spectrum sunblock on two ex vivo skin models*, Photodermatol. Photoimmunol. Photomed. 19(5) (2003), pp. 242–253.

[10] M.C. Lomer, R.P. Thompson, and J.J. Powell, *Fine and ultrafine particles of the diet: Influence on the mucosal immune response and association with Crohn's disease*, Proc. Nutr. Soc. 61(1) (2002), pp. 123–130.

[11] G. Centi, P. Ciambelli, S. Perathoner, and P. Russo, *Environmental catalysis: Trends and outlook*, Catal. Today 75(1–4) (2002), pp. 3–15.

[12] K. Pirkanniemi and M. Sillanpaa, *Heterogeneous water phase catalysis as an environmental application: A review*, Chemosphere 48(10) (2002), pp. 1047–1060.

[13] L. Frazer, *Titanium dioxide: Environmental white knight?* Environ. Health Perspect. 109(4) (2001), pp. A174–177.
[14] K. Hirakawa, M. Mori, M. Yoshida, S. Oikawa, and S. Kawanishi, *Photo-irradiated titanium dioxide catalyzes site specific DNA damage via generation of hydrogen peroxide*, Free Radic. Res. 38(5) (2004), pp. 439–447.
[15] R. Konaka, E. Kasahara, W.C. Dunlap, Y. Yamamoto, K.C. Chien, and M. Inoue, *Ultraviolet irradiation of titanium dioxide in aqueous dispersion generates singlet oxygen*, Redox Rep. 6(5) (2001), pp. 319–325.
[16] D.M. Guldi and M. Prato, *Excited-state properties of C(60) fullerene derivatives*, Acc. Chem. Res. 33(10) (2000), pp. 695–703.
[17] R. Ackroyd, C. Kelty, N. Brown, and M. Reed, *The history of photodetection and photodynamic therapy*, Photochem. Photobiol. 74(5) (2001), pp. 656–669.
[18] A.P. Zhang and Y.P. Sun, *Photocatalytic killing effect of TiO_2 nanoparticles on Ls-174-t human colon carcinoma cells*, World J. Gastroenterol. 10(21) (2004), pp. 3191–3193.
[19] B. Rehn, F. Seiler, S. Rehn, J. Bruch, and M. Maier, *Investigations on the inflammatory and genotoxic lung effects of two types of titanium dioxide: Untreated and surface treated*, Toxicol. Appl. Pharmacol. 189(2) (2003), pp. 84–95.
[20] R. Dunford, A. Salinaro, L.Z. Cai, N. Serpone, S. Horikoshi, H. Hidaka, and J. Knowland, *Chemical oxidation and DNA damage catalysed by inorganic sunscreen ingredients*, Febs. Lett. 418(1–2) (1997), pp. 87–90.
[21] S.M. Hussain, K.L. Hess, J.M. Gearhart, K.T. Geiss, and J.J. Schlager, *In vitro toxicity of nanoparticles in BRL 3A rat liver cells*, Toxicol. In Vitro 19(7) (2005), pp. 975–983.
[22] K.P. Lee, H.J. Trochimowicz, and C.F. Reinhardt, *Pulmonary response of rats exposed to titanium dioxide (TiO_2) by inhalation for two years*, Toxicol. Appl. Pharmacol. 79(2) (1985), pp. 179–192.
[23] A. Aljandali, H. Pollack, A. Yeldandi, Y. Li, S.A. Weitzman, and D.W. Kamp, *Asbestos causes apoptosis in alveolar epithelial cells: Role of iron-induced free radicals*, J. Lab. Clin. Med. 137(5) (2001), pp. 330–339.
[24] G. Oberdorster, J. Ferin, R. Delein, S.C. Soderholm, and J. Finkelstein, *Role of the alveolar macrophage in lung injury: Studies with ultrafine particles*, Environ. Health Perspect. 97 (1992), pp. 193–199.
[25] K. Peters, R.E. Unger, and C.J. Kirkpatrick, *Effects of nano-scaled particles on endothelial cell function in vitro: Studies on viability, proliferation and inflammation*, J. Mater. Sci. Mater. Med. 15(4) (2004), pp. 321–325.
[26] P.S. Gilmour, A. Ziesenis, E.R. Morrison, M.A. Vickers, E.M. Drost, I. Ford, E. Karg, C. Mossa, A. Schroeppel, G.A. Ferron et al., *Pulmonary and systemic effects of short-term inhalation exposure to ultrafine carbon black particles*, Toxicol. Appl. Pharmacol. 195(1) (2004), pp. 35–44.
[27] C. de Haar, I. Hassing, M. Bol, R. Bleumink, and R. Pieters, *Ultrafine but not fine particulate matter causes airway inflammation and allergic airway sensitization to co-administered antigen in mice*, Clin. Exp. Allergy. 36(11) (2006), pp. 1469–1479.
[28] P.C. Maness, S. Smolinski, D.M. Blake, Z. Huang, E.J. Wolfrum, and W.A. Jacoby, *Bactericidal activity of photocatalytic TiO_2 reaction: Toward an understanding of its killing mechanism*, Appl. Environ. Microbiol. 65(9) (1999), pp. 4094–4098.
[29] P.G. Barlow, A. Clouter-Baker, K. Donalson, J. Maccallum, and V. Stone, *Carbon black nanoparticles induce type II epithelial cells to release chemotaxins for alveolar macrophages*, Part. Fibre Toxicol. 2 (2005), p. 11.
[30] C.M. Sayes, R. Wahi, P.A. Kurian, Y. Liu, J.L. West, K.D. Ausman, D.B. Warheit, and V.L. Colvin, *Correlating nanoscale titania structure with toxicity: A cytotoxicity and inflammatory response study with human dermal fibroblasts and human lung epithelial cells*, Toxicol. Sci. 92(1) (2006), pp. 174–185.

[31] K.G. Coonse, A.J. Coonts, E.V. Morrison, and S.J. Heggland, *Cadmium induces apoptosis in the human osteoblast-like cell line Saos-2*, J. Toxicol. Environ. Health A 70(7) (2007), pp. 575–581.
[32] C.C. Daigle, D.C. Chalupa, F.R. Gibb, P.E. Morrow, G. Oberdorster, M.J. Utell, and M.W. Frampton, *Ultrafine particle deposition in humans during rest and exercise*, Inhal. Toxicol. 15(6) (2003), pp. 539–552.
[33] G. Oberdorster, A. Maynard, K. Donalson, V. Castranova, J. Fitzpatrick, K. Ausman, J. Carter, B. Karn, W. Kreyling, D. Lai et al., *Principles for characterizing the potential human health effects from exposure to nanomaterials: Elements of a screening strategy*, Part. Fibre Toxicol. 2 (2005), p. 8.
[34] G.E. Oberdorster, E. Oberdorster, and J. Oberdorster, *Nanotoxicology: An emerging discipline evolving from studies of ultrafine particles*, Environ. Health Perspect. 113(7) (2005), pp. 823–839.
[35] T. Stoeger, C. Reinhard, S. Takenaka, A. Schroeppel, E. Karg, B. Ritter, J. Heyder, and H. Schultz, *Instillation of six different ultrafine carbon particles indicates a surface area threshold dose for acute lung inflammation in mice*, Environ. Health Perspect. 114(3) (2006), pp. 328–333.
[36] S.B. Lovern and R. Klaper, *Daphnia magna mortality when exposed to titanium dioxide and fullerene (C-60) nanoparticles*, Environ. Toxicol. Chem. 25(4) (2006), pp. 1132–1137.
[37] K. Thomas, P. Aguar, H. Kawasaki, J. Morris, J. Nakanishi, and N. Savage, *Research strategies for safety evaluation of nanomaterials, Part VIII: International efforts to develop risk-based safety evaluations for nanomaterials*, Toxicol. Sci. 92(1) (2006), pp. 23–32.
[38] K. Thomas and P. Sayre, *Research strategies for safety evaluation of nanomaterials, part I: Evaluating the human health implications of exposure to nanoscale materials*, Toxicol. Sci. 87(2) (2005), pp. 316–321.
[39] R. Elo, K. Maatta, E. Uksila, and A.U. Arstila, *Pulmonary deposits of titanium dioxide in man*, Arch. Pathol. 94(5) (1972), pp. 417–424.
[40] L.E. Rode, E.M. Ophus, and B. Gylseth, *Massive pulmonary deposition of rutile after titanium dioxide exposure: Light-microscopical and physico-analytical methods in pigment identification*, Acta Pathol. Microbiol. Scand. [A] 89(6) (1981), pp. 455–461.
[41] J. Park, S. Bayer, K. Von der Mark, and P. Schmuki, *Nanosize and vitality: TiO_2 nanotube diameter directs cell fate*, Nano. Lett. 7(6) (2007), pp. 1686–1691.
[42] J.J. Wang, B.J. Sanderson, and H. Wang, *Cyto- and genotoxicity of ultrafine TiO_2 particles in cultured human lymphoblastoid cells*, Mutat. Res. 628(2) (2007), pp. 99–106.
[43] J.M. Veranth, C.A. Reilly, M.M. Veranth, T.A. Moss, C.R. Langelier, D.L. Lanza, and G.S. Yost, *Inflammatory cytokines and cell death in BEAS-2B lung cells treated with soil dust, lipopolysaccharide, and surface-modified particles*, Toxicol. Sci. 82(1) (2004), pp. 88–96.
[44] D.W. Kamp, V. Panduri, S.A. Weitzman, and N. Chandel, *Asbestos-induced alveolar epithelial cell apoptosis: Role of mitochondrial dysfunction caused by iron-derived free radicals*, Mol. Cell Biochem. 234-235(1-2) (2002), pp. 153–160.
[45] M. Thibodeau, C. Giardina, and A.K. Hubbard, *Silica-induced caspase activation in mouse alveolar macrophages is dependent upon mitochondrial integrity and aspartic proteolysis*, Toxicol. Sci. 76(1) (2003), pp. 91–101.
[46] T. Xia, M. Kovochich, J. Brant, M. Hotze, T. Oberley, C. Sioutas, J.I. Yeh, M.R. Wiesner, and A.E. Nel, *Comparison of the abilities of ambient and manufactured nanoparticles to induce cellular toxicity according to an oxidative stress paradigm*, Nano Lett. 6(8) (2006), pp. 1794–1807.
[47] L.G. Gutwein and T.J. Webster, *Increased viable osteoblast density in the presence of nanophase compared to conventional alumina and titania particles*, Biomaterials 25(18) (2004), pp. 4175–4183.
[48] M. Cho, H. Chung, W. Choi, and J. Yoon, *Linear correlation between inactivation of E. coli and OH radical concentration in TiO_2 photocatalytic disinfection*, Water Res. 38(4) (2004), pp. 1069–1077.
[49] A. Churg, B. Stevens, and J.L. Wright, *Comparison of the uptake of fine and ultrafine TiO_2 in a tracheal explant system*, Am. J. Physiol. 274(1 Pt 1) (1998), pp. L81–86.

[50] H.A. Jeng and J. Swanson, *Toxicity of metal oxide nanoparticles in mammalian cells*, J. Environ. Sci. Health. A Tox. Hazard Subst. Environ. Eng. 41(12) (2006), pp. 2699–2711.
[51] J.F. Kerr, A.H. Wyllie, and A.R. Currie, *Apoptosis: A basic biological phenomenon with wide-ranging implications in tissue kinetics*, Br. J. Cancer 26(4) (1972), pp. 239–257.
[52] E. Dopp, J. Saedler, H. Stopper, D.G. Weiss, and D. Schiffmann, *Mitotic disturbances and micronucleus induction in Syrian hamster embryo fibroblast cells caused by asbestos fibers*, Environ. Health Perspect. 103(3) (1995), pp. 268–271.
[53] E. Dopp, B. Nebe, C. Hahnel, T. Papp, B. Alonso, M. Simko, and D. Schiffmann, *Mineral fibers induce apoptosis in Syrian hamster embryo fibroblasts*, Pathobiology 63(4) (1995), pp. 213–221.